SUPPLEMENTAL INFORMATION

DELFT 3-D MODELING: MODEL DESIGN, SETUP, AND ANALYSIS

Each experiment starts from the initial condition of a straight channel 10 km long, with an adjacent 3300 m wide floodplain (Figure DR1). The floodplain is separated from the channel by a levee 400 m wide, 3 m tall, and 10 km long. Both the channel and floodplain have the same slope of 5×10^{-4}. The initial cross-sectionally averaged width and depth of the channel are 250 m and 3 m, respectively, chosen to be in equilibrium with the bankfull discharge. The channel has a normalized super-elevation (levee height divided by channel depth) of 1 to insure that avulsions occur in each simulation. To simulate nonuniform floodplain topography we randomly place Gaussian-shaped, non-overlapping bumps, each ~0.5 m high and 150 m x 150 m in area, over 50% of the floodplain area. Tests showed that model results are generally insensitive to a range of bump heights (0.25-1.0 m) and percent coverage (30-80%).

All runs employ a morphodynamic scale factor of 20. This scale factor is a multiplicative term applied to the erosive or depositional fluxes to/from the bed and is intended to speed up the computation. We tested sensitivity to this parameter and found our results to be insensitive to a value of 20 or less. The incoming flood hydrograph has a high-flow (1900 $m^3 s^{-1}$), low-flow (330 $m^3 s^{-1}$), and bankfull (750 $m^3 s^{-1}$) discharge. The hydrograph is modeled such that each flood is 5 days long (when accounting for the scale factor). Because little morphodynamic change happens at low flow we minimize the length of time between floods. In our runs there are 10 days between each flood, which is enough time to allow for the floodplain to completely drain before the next flood arrives. The channel and floodplain have the same hydraulic roughness with $C = 65\ m^{1/2} s^{-1}$.

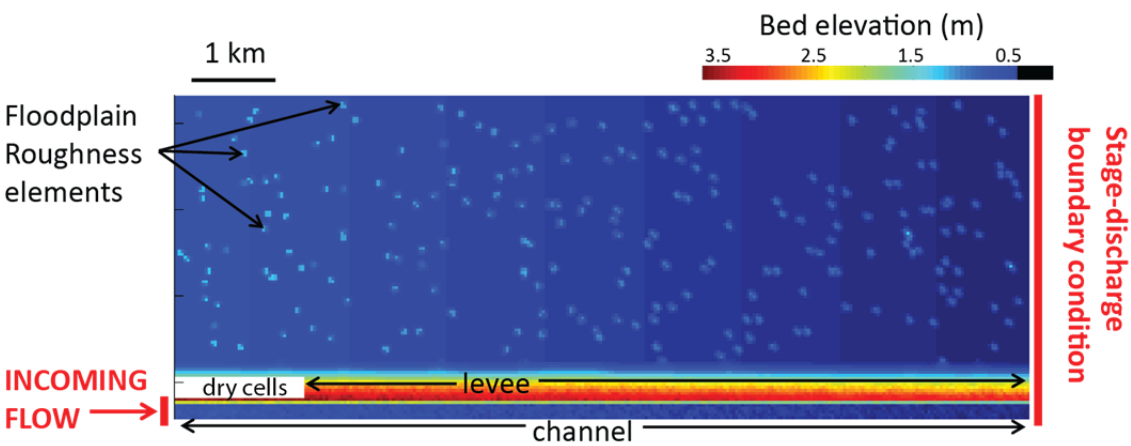

Figure DR1: Planview of model set up. Flow and sediment boundary conditions are specified at the incoming flow boundary, while stage discharge relations are specified downstream. Levee cells closest to the incoming flow boundary are set to 'dry' so that the avulsion does not occur close to the boundary creating instabilities.

R is directly observed in each model run. To calculate T_p we track the front of the advancing sediment wedge through time, and L_p is the distance from the avulsion breakout to the end of the model domain. We calculate T_i directly by averaging incision rates at randomly sampled floodplain locations that are experiencing incision (i.e. we ignore areas undergoing no change). We assume D_c is equal to ½ of depth of the parent channel (e.g., superelevation thresholds of Mohrig et al., 2000), and measured the spatial distribution of incision and found that $\alpha \approx 0.5$.

Table DR1: Results from each model run in this study.

Run Number	Grain Size of sand fraction	$\tau_{c(mud)}$	Areal percentage of floodplain that is sand	Alpha	D_c	$\bar{P}$	$\bar{I}$	T_p (days)	T_i (days)	R
A3	75	0.275	71	0.5	1.5	8.37E-05	2.52E-08	1065	1379	1.30
B2	125	0.185	78	0.5	1.5	8.57E-05	2.37E-08	1053	1463	1.39
B3	125	0.275	73	0.5	1.5	8.44E-05	2.08E-08	1015	1669	1.64
C1	250	0.1	47	0.5	1.5	4.08E-05	3.89E-08	2323	893	0.38
C2	250	0.185	58	0.5	1.5	4.86E-05	2.02E-08	1952	1723	0.88
C3	250	0.275	53	0.5	1.5	4.28E-05	2.09E-08	2216	1659	0.75
D1	750	0.1	15	0.5	1.5	1.62E-05	6.69E-08	5286	519	0.10
D2	750	0.185	23	0.5	1.5	2.31E-05	3.79E-08	3750	917	0.24
D3	750	0.275	28	0.5	1.5	2.83E-05	3.12E-08	3150	1113	0.35

DATA FROM ANCIENT DEPOSITS

Classifying Avulsion Stratigraphy

Avulsion stratigraphy surrounding channel-belt sand bodies in well-exposed outcrop belts was observed in the Ferris and Willwood formations and Shire Member of the Wasatch Formation. Avulsion stratigraphy was classified as either *stratigraphically transitional* or *stratigraphically abrupt* following Jones and Hajek (2007). Floodplain deposits subjacent to *stratigraphically transitional* channel-belt deposits show generally progradational successions with evidence of increasing sedimentation rates up-section, including, for example, more, coarser, and/or thicker crevasse-splay deposits and weaker paleosol development than seen in characteristic distal or far-field floodplain deposits. *Stratigraphically abrupt* channel-belt deposits are juxtaposed directly atop distal floodplain deposits with no evidence for intervening proximal-overbank deposition. We note that channel enlargement upon successful avulsion can lead to the partial erosion of underlying proximal-overbank deposits (e.g., Smith et al., 1989); consequently we only include sand bodies where both channels and adjacent floodplain deposits are extensively exposed in outcrop.

Figure DR2 shows an example section through two Shire Member channel deposits. Tables DR2-DR4 summarize data for observations from each unit, including the maximum channel-deposit grain size and the maximum grain size of floodplain deposits beneath the channel deposit (typically within approximately one channel-belt thickness beneath the channel deposit). Note that for the Shire Member and Willwood Formation, channel grain-size observed in hand samples approximates the median grain diameter (D50) of bed material. The Ferris Formation D50 of all channels is 1-2 mm, but some channels contain rare pebbles and cobbles (Hajek et al., 2012). Other sedimentological characteristics of each unit are described in the following sections.

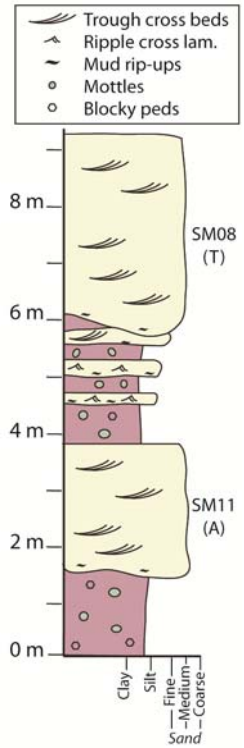

Figure DR2 (left). Example measured section from Shire Member channel deposits SM11 and SM08. SM11 is a stratigraphically abrupt deposit (A) with a maximum grain size of silt beneath the channel. SM08 is a stratigraphically transitional avulsion deposit (T) with sandy crevasse-splay deposits beneath the channel.

Figure DR3 (right). Map of portions of Wyoming and Colorado, USA showing channel-deposit localities from this study: the Willwood Formation (red, Bighorn Basin, WY), Ferris Formation (yellow, Hanna Basin, WY), and Shire Member of the Wasatch Formation (blue, Piceance Basin, CO). Map available at https://mapsengine.google.com/map/edit?mid=zyZWlaO26o9g.k_Mm6yNohDFg

Field Areas

Shire Member of the Wasatch Formation

The Eocene Shire Member of the Wasatch Formation is a fluvial unit exposed in the Piceance Basin, western Colorado (Foreman et al., 2012; Lorenz and Nadon, 2002; Figure DR4). The Shire Member is characterized by dominantly medium-sand channel-belt deposits and silt-and-clay-rich floodplain mudstones with moderate- to well-developed paleosol horizons (e.g., Foreman et al., 2012; Mohrig et al., 2000). Data presented here were collected during 2011 and 2012.

Table DR2: Data for Shire Member observations. T = Transitional avulsion stratigraphy, A = stratigraphically abrupt avulsion stratigraphy. Channel grain size abbreviations indicate sand-class size (F = fine, M = medium, modified by upper (U) or lower (L).

ID	Latitude	Longitude	Channel grain size	Max. overbank grainsize beneath channel	Avulsion stratigraphy
SM01	39° 26′ 35.68″	-108° 15′ 5.966″	FU-ML	Fine sand	T
SM02	39° 30′ 22.2″	-108° 7′ 25.9″	FU	Fine sand	A
SM03	39° 30′ 22.2″	-108° 7′ 25.9″	ML	Silt	A
SM04	39° 30′ 22.2″	-108° 7′ 25.9″	FL	Very-fine sand	T
SM05	39° 23′ 33.7″	-108° 7′ 50.1″	FL	Very-fine sand	T
SM06	39° 24′40.8″	-108° 5′55.3″	ML	Fine sand	T
SM07	39° 24′43″	-108° 5′52″	FU	Fine sand	T
SM08	39° 24′43.7″	-108° 5′52.6″	FU-ML	Fine sand	T
SM09	39° 24′ 42.7″	-108° 5′ 52.5″	FL-FU	Very-fine sand	T
SM10	39° 21′ 4.575″	-108° 26′ 12.104″	FU	Silt	A
SM11	39° 24′ 43.7″	-108° 5′ 52.6″	LM-UM	Silt	A
SM12	39.45519696	-108.351558	FU	Silt	T
SM13	39.29978902	-108.155527	FU	Silt	A
SM14	39.29813996	-108.156232	ML	Fine sand	T
SM15	39.29913397	-108.144515	FU	Silt	A
SM16	39.39923099	-108.119842	FU	Fine sand	T
SM17	39.399491	-108.121813	ML	Silt	A
SM18	39.37534198	-108.186428	ML	Silt	A
SM19	39.38143303	-108.183276	FU	Silt	A
SM20	39.38171298	-108.183181	MU	Fine sand	T
SM21	39.28972101	-108.161193	ML-FU	Silt	A
SM22	39.27737899	-108.159178	FL-ML	Fine sand	T
SM23	39.39936401	-108.120666	FU	Fine sand	T

Willwood Formation

The Paleocene-Eocene Willwood Formation is exposed in the Bighorn Basin, Wyoming (Figure DR3) and comprises medium-to-coarse-sand channel deposits set in clay-rich floodplain-mudstone deposits with prominent paleosol horizons (e.g., Kraus, 2001; Kraus and Wells, 1999). Avulsion stratigraphic data come from Jones (2007) and Jones and Hajek (2007). Note that only deposits of trunk channels (c.f. Kraus) are included in this analysis.

Table DR3: Data for Willwood Formation observations. T = transitional avulsion stratigraphy, A = stratigraphically abrupt avulsion stratigraphy.

ID	Latitude	Longitude	Channel grain size	Max. overbank grainsize beneath channel	Avulsion stratigraphy
WW01	N44º19'07.0"	W108º21'25.2"	Medium sand	Silt	A
WW02	N44º19'07.0"	W108º21'25.2"	Medium sand	Fine sand	T
WW03	N44º19'07.0"	W108º21'25.2"	Fine sand	Very-fine sand	T
WW04	N44º19'17.8"	W108º21'23.3"	Medium sand	Silt	A
WW05	N44º20'40.4"	W108º41'14.5"	Medium sand	Fine sand	T
WW06	N44º22'56.9"	W108º38'38.8"	Medium sand	Very-fine sand	T
WW07	N44º23'10.0"	W108º37'20.5"	Medium sand	Very-fine sand	T
WW08	N44º23'10.0"	W108º37'20.5"	Medium sand	Very-fine sand	T
WW09	N44º23'10.0"	W108º37'20.5"	Medium sand	Very-fine sand	T
WW10	N44º23'25.3"	W108º33'44.6"	Medium sand	Silt	A
WW11	N44º23'25.3"	W108º33'44.6"	Fine sand	Very-fine sand	T
WW12	N44º23'25.3"	W108º33'44.6"	Medium sand	Silt	T
WW13	N44º22'09.0"	W108º35'56.0"	Fine sand	Very-fine sand	T
WW14	N44º22'09.0"	W108º35'56.0"	Fine sand	Silt	T
WW15	N44º22'09.0"	W108º35'56.0"	Medium sand	Silt	T
WW16	N44º21'32.0"	W108º35'54.0"	Fine sand	Very-fine sand	T
WW17	N44º21'32.0"	W108º35'54.0"	Fine sand	Silt	T
WW18	N44º21'13.0"	W108º35'46.0"	Fine sand	Very-fine sand	T
WW19	N44º22'14.0"	W108º35'50.0"	Fine sand	Very-fine sand	T
WW20	N44º22'47.0"	W108º33'54.0"	Medium sand	Very-fine sand	T
WW21	N44º22'28.0"	W108º33'50.0"	Medium sand	Very-fine sand	T
WW22	N44º25'00.0"	W108º29'43.0"	Fine sand	Very-fine sand	T
WW23	N44º25'00.0"	W108º29'43.0"	Medium sand	Fine sand	T
WW24	N44º34'09.0"	W108º46'47.0"	Medium sand	Fine sand	T
WW25	N44º34'09.0"	W108º46'47.0"	Medium sand	Fine sand	T
WW26	N44º34'09.0"	W108º46'47.0"	Coarse sand	Fine sand	T
WW27	N44º34'09.0"	W108º46'47.0"	Medium sand	Fine sand	T
WW28	N44º34'09.0"	W108º46'47.0"	Fine sand	Fine sand	T

Ferris Formation

The Maastrictian/Paleocene Ferris Formation crops out in the northern Hanna Basin, Wyoming (Figure DR3), where it dips nearly 80º to the south, exposing a cross-section of the paleo-basin fill across the present-day land surface (Hajek et al., 2012; Hajek et al., 2010). Channel-belt sand bodies primarily comprise coarse sand and are surrounded by very clay-rich, carbonaceous floodplain mudstone deposits. Avulsion stratigraphy data presented here was documented during channel mapping (Hajek, 2009), when individual channel bases were tracked along the outcrop exposure.

Table DR4: Data for Ferris Formation observations. T = transitional avulsion stratigraphy, A = stratigraphically abrupt avulsion stratigraphy. Note that channel grain size for the Ferris Formation represents the *maximum* observed grain size in mm, including measurement from small numbers of pebbles and cobbles found within some sand bodies (from Hajek et al., 2012). Ferris channel bed-material deposits comprise dominantly 1-2 mm sand.

ID	Latitude	Longitude	Channel grain size (maximum, mm)	Max. overbank grain size beneath channel	Avulsion stratigraphy
FF01	360812.3718	4655704.123	30.5	Silt	A
FF02	360771.9189	4655763.616	1	Silt	A
FF03	360891.0615	4655775.911	2	Silt	A
FF04	360782.5696	4655811.619	12.5	Silt	A
FF05	360591.7655	4655774.059	1	Silt	A
FF06	360761.541	4655643.863	1	Silt	A
FF07	360716.5606	4655640.596	32.5	Silt	A
FF08	360629.0996	4655650.347	1	Silt	A
FF09	360636.0641	4655655.527	1	Silt	A
FF10	360643.457	4655612.66	10.8	Silt	A
FF11	359751.6297	4655959.687	9.4	Silt	A
FF12	359809.3444	4655964.406	1	Silt	A
FF13	359852.6509	4655955.673	1	Silt	A
FF14	360066.8111	4655938.87	17	Silt	A
FF15	359968.3555	4655931.616	73	Silt	A
FF16	360457.2558	4655914.322	1	Silt	A
FF17	359690.8469	4655699.563	28.5	Silt	A
FF18	359874.2538	4655930.354	1	Silt	A
FF19	359696.5197	4655938.942	1	Silt	A
FF20	359640.4499	4655947.747	1	Silt	A
FF21	360329.7802	4655860.472	65	Silt	A
FF22	359878.1719	4655856.17	1	Silt	A
FF23	359894.7191	4655862.364	1	Silt	A
FF24	360135.2187	4655850.192	6.4	Silt	A
FF25	360080.5708	4655862.362	24	Silt	A
FF26	360044.1773	4655874.177	1	Silt	A

FF27	360612.2953	4655853.037	2	Silt	A
FF28	360488.0496	4655840.793	1	Silt	A
FF29	360431.861	4655877.421	1	Silt	A
FF30	360145.3805	4655884.151	1	Silt	A
FF31	360070.3494	4655888.529	1	Silt	A
FF32	360341.0133	4655831.359	3.6	Silt	A
FF33	360574.5935	4655787.053	1	Silt	A
FF34	360471.2401	4655800.562	2	Silt	A
FF35	360483.4888	4655806.76	1	Silt	A
FF36	360287.2239	4655823.324	8.6	Silt	A
FF37	360558.5549	4655806.565	10.2	Silt	A
FF38	360408.775	4655823.056	1	Silt	A
FF39	360740.8255	4655793.288	22.5	Silt	A
FF40	360681.8697	4655805.509	4	Silt	A
FF41	360682.0209	4655725.671	9.8	Medium Sand	T
FF42	360710.3073	4655719.736	1	Silt	A
FF43	360696.9181	4655715.582	1	Silt	A
FF44	360774.1262	4655711.049	10	Silt	A
FF45	360743.5516	4655886.913	2.45	Silt	A
FF46	360704.0721	4655884.632	16.5	Silt	A
FF47	360612.4799	4655905.557	18.2	Silt	A
FF48	360665.7065	4655896.28	1	Silt	A
FF49	360576.623	4655898.555	16.4	Silt	A
FF50	360296.229	4655800.911	1	Silt	A
FF51	360351.9842	4655784.993	1	Silt	A
FF52	360047.5048	4655821.1	1	Silt	A
FF53	359968.8825	4655827.426	1	Silt	A
FF54	360142.2351	4655805.789	37.5	Silt	A
FF55	360130.4903	4655789.853	1	Silt	A
FF56	360632.8349	4655678.771	35.5	Silt	A
FF57	360674.8638	4655675.115	22	Silt	A
FF58	360742.3496	4655670.981	1	Silt	A
FF59	360672.6401	4655580.734	2	Silt	A
FF60	360580.7354	4655580.396	1	Silt	A
FF61	360639.9687	4655589.741	1	Silt	A
FF62	360359.5092	4655601.344	1	Silt	A
FF63	360309.6134	4655647.276	1	Silt	A
FF64	359688.7242	4655752.015	10.4	Silt	A
FF65	359755.9648	4655733.029	1	Silt	A
FF66	359455.9268	4655787.85	1	Silt	A
FF67	359718.9214	4655765.644	35	Silt	A

FF68	359593.8699	4655780.61	1	Silt	A
FF69	359610.0888	4655783.331	1	Silt	A
FF70	360006.461	4655749.048	7	Silt	A
FF71	360457.8563	4655710.8	40.2	Silt	A
FF72	360340.9268	4655681.5	8.5	Silt	A
FF73	360285.9698	4655661.365	1	Silt	A
FF74	360459.2461	4655688.895	1	Silt	A
FF75	360159.6712	4655718.159	66	Silt	A
FF76	360137.7578	4655715.024	1	Silt	A
FF77	359780.285	4655832.92	19.5	Silt	A
FF78	359774.6344	4655816.136	16.9	Silt	A
FF79	359785.4666	4655796.966	2	Silt	A
FF80	360353.428	4655699.517	1	Silt	A
FF81	360257.4321	4655700.866	34.5	Medium Sand	T

REFERENCES

Foreman, B. Z., Heller, P. L., and Clementz, M. T., 2012, Fluvial response to abrupt global warming at the Palaeocene/Eocene boundary: Nature, v. 491, p. 92-95.

Hajek, E. A., 2009, Characterizing and interpreting channel-body clustering in the Ferris Formation, Hanna Basin, Wyoming [PhD dissertation] University of Wyoming, 201 p.

Hajek, E. A., Heller, P. L., and Schur, E. L., 2012, Field test of autogenic control on alluvial stratigraphy (Ferris Formation, Upper Cretaceous–Paleogene, Wyoming): GSA Bulletin, v. 124, no. 11-12, p. 1898-1912.

Hajek, E. A., Heller, P. L., and Sheets, B. A., 2010, Significance of channel-belt clustering in alluvial basins: Geology, v. 38, no. 6, p. 535-538.

Jones, H. L., 2007, Characterizing Ancient Avulsion Stratigraphy and its Significance [PhD dissertation] University of Wyoming, 230 p.

Jones, H. L., and Hajek, E. A., 2007, Characterizing avulsion stratigraphy in ancient alluvial deposits: Sedimentary Geology, v. 202, no. 1-2, p. 124-137.

Kraus, M. J., 2001, Sedimentology and depositional setting of the Willwood Formation in the Bighorn and Clark's Fork basins: Papers on Paleontology, v. 33, p. 15-28.

Kraus, M. J., and Wells, T. M., 1999, Recognizing avulsion deposits in the ancient stratigraphical record, *in* Smith, N. D., and Rogers, J., eds., Fluvial Sedimentology VI, Volume 28, International Association of Sedimentologists, Special Publication 28, p. 251-268.

Lorenz, J. C., and Nadon, G. C., 2002, Braided-river deposits in a muddy depositional setting; the Molina Member of the Wasatch Formation (Paleogene), west-central Colorado, U.S.A: Journal of Sedimentary Research, v. 72, no. 3, p. 376-385.

Mohrig, D., Heller, P. L., Paola, C., and Lyons, W. J., 2000, Interpreting avulsion process from ancient alluvial sequences; Guadalope-Matarranya system (northern Spain) and Wasatch Formation (western Colorado): Geological Society of America Bulletin, v. 112, no. 12, p. 1787-1803.

Smith, N. D., Cross, T. A., Dufficy, J. P., and Clough, S. R., 1989, Anatomy of an avulsion: Sedimentology, v. 36, p. 1-23.